

# A Comparison of the Photoelectric Current Responses Resulting from the Proton Pumping Process of Bacteriorhodopsin under Pulsed and CW Laser Excitations

Jian-ping Wang, Li Song, Seoung-kyo Yoo, and Mostafa A. El-Sayed\*

School of Chemistry and Biochemistry, Georgia Institute of Technology, Atlanta, Georgia 30332-0400

Received: July 29, 1997; In Final Form: September 29, 1997<sup>®</sup>

When excited with a pulsed laser, an electric field-oriented bacteriorhodopsin (bR) film on an indium–tin oxide (ITO) conductive electrode generates a photocurrent composed of at least three different components: B1 (<100 ps), B2 (~60  $\mu$ s), and B3 (~ms). When excited with an electronic shutter modulated CW light pulse (>200 ms in duration), a differential photocurrent (components D1 and D2 with decay times in milliseconds) is observed from the bR film. D1 is observed when the CW light is turned on, and D2 is observed when the CW light is turned off. In this paper, we compare the amplitudes and lifetimes of B2, B3, and D1 at various values of pH and ionic strength of the electrolyte solution in which the photocurrent is measured. It is found that changing the film orientation changes the polarity (sign) of B1 and B2, while it does not affect the polarity of B3 and D1. It is also found that B3 and D1 change their polarity upon changing the pH of electrolyte solution, whereas B1 and B2 do not. These results suggest that the origin of B3 and D1 is different from that of B1 and B2. Our results suggest that B3 and D1 are due to the formation of a transient proton capacitor between the two ITO electrodes resulting from the proton pumping in bR. The magnitude and sign of B3 and D1 are determined by the transient proton concentration change (accumulation or disappearance) occurring near the bR-modified ITO electrode interface on the millisecond time scale. The change of sign in B3 and D1 as a function of pH is due to the sequence of proton release/uptake in the bR photocycle: It first releases protons into the aqueous solution at high pH, while it first takes up protons from the aqueous solution at low pH. The effects of buffer and ionic strength on B3 and D1 are discussed in terms of the kinetics of proton release/uptake and of the transportation of positive and negative ions in the electrolyte solution.

## 1. Introduction

Bacteriorhodopsin (bR) is the only protein located in the purple membrane (PM) of *Halobacterium salinarum*. bR pumps protons across its membrane upon the absorption of light.<sup>1</sup> The vectorial proton translocation from the cytoplasmic side to the extracellular side builds up an electrochemical potential across the membrane, providing energy for the synthesis of ATP from ADP. The retinal chromophore of bR is attached to the protein via a protonated Schiff base (PSB) at the  $\epsilon$ -amino group of the Lys-216 residue. The photochemistry of bR has been extensively studied in the past three decades.<sup>2–5</sup> However, the molecular mechanism of proton pump in bR has not been completely understood.

Photoelectric studies have provided fruitful information for the understanding of the proton pumping mechanism in bR.<sup>6–10</sup> The photocurrent of bacteriorhodopsin induced by a pulsed laser has been extensively studied, and several components have been identified.<sup>7–10</sup> The first component (B1) is ultrafast, with a rise time less than 100 ps. B1 is thought to originate from the charge separation as the result of retinal photoisomerization from *all-trans* to 13-*is* in bR.<sup>7,11</sup> This model is supported by the fact that B1 is not observed for modified *all-trans*-retinal which cannot isomerize.<sup>12</sup> The second component (B2) has a decay lifetime of 40–100  $\mu$ s. B2 is thought to be due to the vectorial proton translocation from the Schiff base to the counterion or due to proton release from an unknown proton-releasing group to solution. Since B2 and B1 are in opposite directions, it was proposed<sup>7</sup> that the proton transfer in bR undergoes a slingshot type of mechanism in which a proton first recoils and then

advances in the direction of vectorial transport. Under certain conditions (normal pH, moderate ionic strength), the decay of the photovoltage corresponding to B2 was found to have a similar lifetime as the formation of the M intermediate from oriented PM sheets in aqueous suspension.<sup>13</sup> Discrepancies exist, however, in the lifetimes of B2 observed from different laboratories.<sup>8</sup> Under high ionic strength condition (such as >40 mM KCl), a good correlation between the decay lifetime of B2 and the lifetime of M formation in the pH range from 2.4 to 11.0 was reported.<sup>9</sup>

On the millisecond time scale, a slower photocurrent component (B3) has also been observed.<sup>6,7,9,10,13–16</sup> Previous studies on B3, however, have provided little understanding of its origin and factors that affect its magnitude and lifetime. A common observation for B3 is that it is slower than B2, with a small amplitude near neutral pH. For example, in the time scale of 50 ms, the observed B3 from oriented bR in a poly(acrylamide) gel, immersed in 5 mM CaCl<sub>2</sub> at neutral pH, was about 30 times weaker in amplitude compared to B2.<sup>9</sup> It is possible that B3 originates from different processes, e.g., slow charge-transfer events after the formation of M, the release or uptake of protons or other ions occurring on the surface of bR membrane, concomitant transient dipole moment change, or even secondary ionic events.

When excited with a modulated CW light pulse, a differential photocurrent (components D1 and D2 with decay times in milliseconds) is observed from the bR film. D1 is observed when the CW light is turned on, and D2 is observed when the CW light is turned off. The differential photocurrent from oriented bR has been studied previously.<sup>17–20</sup> Robertson and Lukashev<sup>20</sup> have shown conclusively that the differential photocurrent from bR is due to rapid pH change and not to

\* To whom correspondence should be addressed.

<sup>®</sup> Abstract published in *Advance ACS Abstracts*, November 1, 1997.

charge displacement. Recently, in a short communication,<sup>16</sup> we presented results that suggest that D1 in the differential photocurrent (observed when a CW light source is turned on) and B3 (observed under pulsed laser excitation) both have the same molecular origin. We further proposed that it is the change in the proton concentration near the membrane-ITO interface that can account for the observed photocurrent. In this paper, we report the effects of pH, buffer, and ionic strength on B3 and D1. The results support our previous proposal<sup>16</sup> that the molecular origins of B3 and D1 are the same and can be ascribed to the change in the proton concentration near the bR-ITO electrode interface. An increase in proton concentration produces a positive B3 and D1 while a decrease in proton concentration produces a negative B3 and D1.

## 2. Materials and Methods

Purple membrane was prepared from the wild-type *Halo-bacterium salinarium* strain ET1001, using a standard procedure described previously.<sup>21</sup> Purified bacteriorhodopsin was washed four times with centrifugation using doubly deionized water (DDW, resistance 18 M $\Omega$ -cm) and was then suspended in DDW with a final concentration of 30–50  $\mu$ M. The purple membrane was oriented onto the ITO conductive electrode by their permanent dipole moment under an external electric field, achieved by the electrophoretic sedimentation method.<sup>16,22,23</sup> Oriented bR film can be prepared with either the cytoplasmic (CP) or the extracellular (EC) surface facing the ITO by controlling the pH of the bR suspension.<sup>16</sup> The bR film we used in this study was mostly oriented with the extracellular (EC) side facing the ITO (orientation pattern is ITO/EC-CP), and its orientation was confirmed by the polarity of B1 and B2. The absorbance of the film was in the range 0.1–1.0 at  $\lambda = 570$  nm. The photocurrent from each of the oriented bR films did not deteriorate significantly over time.

The ITO electrode, deposited with a oriented bR film, was placed in a  $10 \times 10 \times 45$  mm cuvette with a blank ITO electrode separated 6–8 mm away. Both of the working electrode (bR-containing ITO) and the reference electrode (blank ITO) were immersed in an electrolyte solution. The photocurrent was measured by connecting the working electrode to the positive input and the reference electrode to the negative input of a Keithley current amplifier (Model 428).<sup>16</sup> In the pulsed laser excitation measurement, the sample was excited by the second harmonic (532 nm) of a Q-switched Nd:YAG laser (Quanta-Ray, DCR-3, Spectra Physics) with an intensity of  $\sim 10$  mJ and a pulse width of 10 ns. In the modulated CW excitation measurement, the light source was either a xenon lamp (100 W) equipped with long pass filters to pass light with  $\lambda > 500$  nm or a CW dye laser (Innova 70, Coherent) tuned to 570 nm. Modulation of the CW light was introduced by an electronic shutter which was controlled by a computer. The rise time of the shutter was typically  $\sim 0.3$  ms. The open time of the shutter was controlled from  $\sim 200$  ms to  $\sim 1$  s. A positive photocurrent represents the direction of positive charge moving from the working electrode via the current meter to the reference electrode. Data acquisition was synchronized with either the laser flash or the operating voltage on the electronic shutter and controlled by a PC computer. Typically, the photocurrent was averaged over 10–50 laser pulses or shutter modulations to obtain a good signal-to-noise ratio.

## 3. Results

**3.1. Photocurrent on Different Time Scales.** Figure 1 shows the photocurrent from an oriented bR film measured in an aqueous solution of 10 mM KCl and 2 mM K<sub>2</sub>HPO<sub>4</sub> (pH

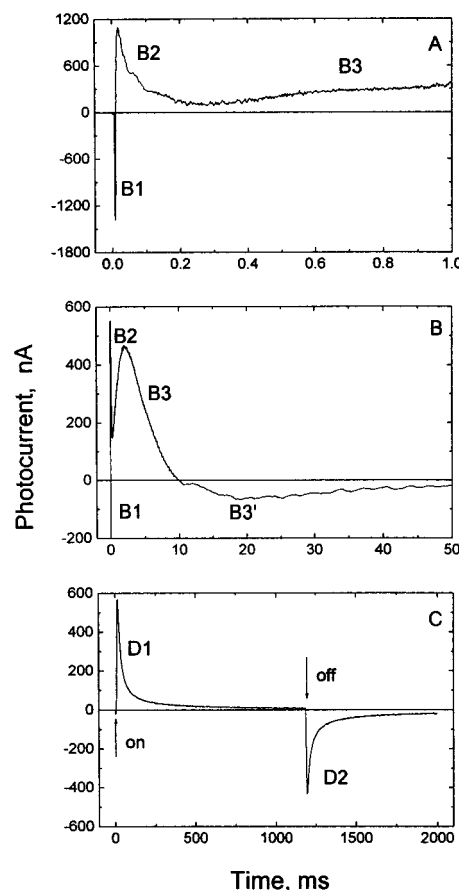


**Figure 1.** Photocurrent observed on the micro-millisecond time scales from an oriented bR film in 10 mM KCl, 2 mM K<sub>2</sub>HPO<sub>4</sub> at pH = 8.0 and room temperature. The sample was excited with a 10 ns pulsed laser (A and B) and with a modulated CW excitation (C). (A) B1 and B2 on the time scale of 0.5 ms, under pulsed laser excitation. (B) B3 and B3' on the 50 ms time scale, under pulsed laser excitation. (C) D1 and D2, upon turning on and turning off the CW light source.

8.0), on different time scales. Under pulsed laser excitation, the very fast component (B1) and the microsecond component (B2) are both shown in Figure 1A. These results are consistent with those obtained previously for bilayer lipid membrane (BLM) supported bR film<sup>24</sup> and from oriented bR immobilized in poly(acrylamide) gel.<sup>9</sup> A slower component (B3) is observed on the millisecond time range (shown in Figure 1B) in which B1 and B2 are not very well resolved. It should be noted that, at this pH, B3 has the same sign as B2, which is opposite to B1. In addition, the rise and decay of B3 is much slower compared to B2 (see following sections). After B3 decays to zero, a negative component B3' appears after  $\sim 10$  ms. Under modulated CW illumination, the differential photocurrent (D1 and D2) is shown in Figure 1C. The positive photocurrent corresponds to turning on the CW light source, and the negative peak corresponds to turning the light off.

Figure 2 gives various photocurrent components under identical experimental conditions as Figure 1, except that pH is 3.0. From Figure 1 and Figure 2, it can be seen that B1 and B2 do not change their sign as the pH is changed. The amplitudes of both B1 and B2 change slightly as the pH changes. This result agrees with a previous study.<sup>9</sup> The observed deformation of the decay of B2 within the time domain in Figure 2A is a result of the overlap with the B3 rise as shown in Figure 2B. B3 and D1 both change their polarity (sign) as the pH is decreased from 8.0 to 3.0, with a positive sign at high pH (8.0) and negative at low pH (3.0). The polarity of B3 is always the same as D1, although B3 and D1 are obtained under different

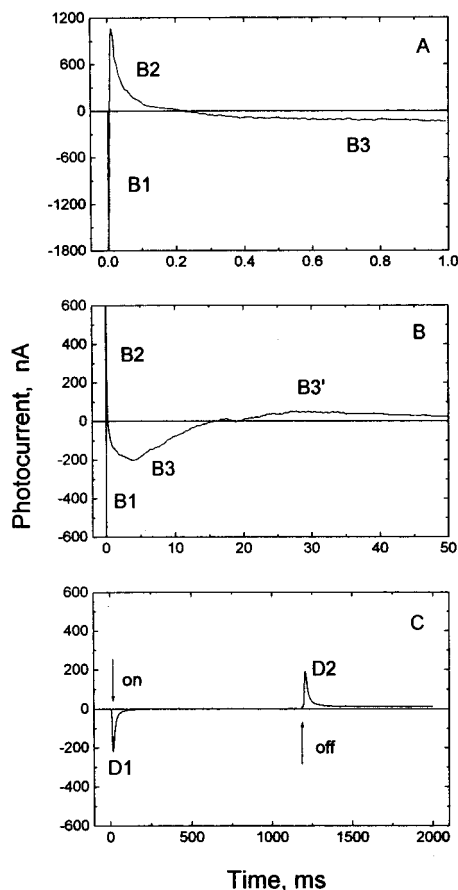
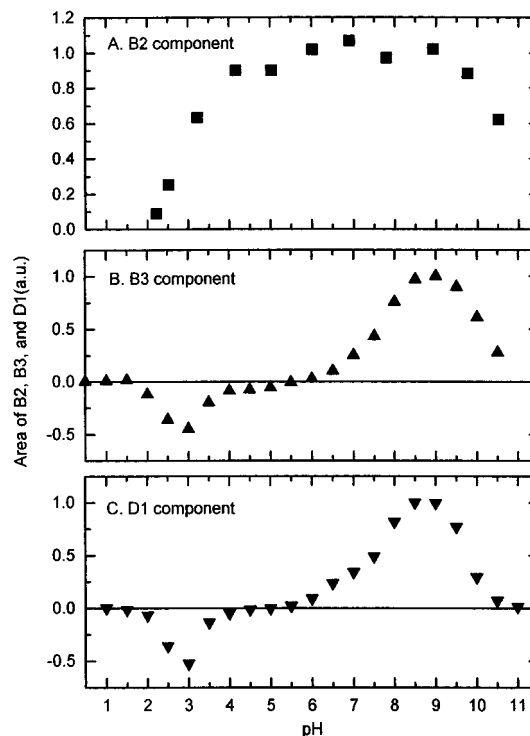


**Figure 2.** Photocurrent signals with conditions identical with that in Figure 1, except that the pH is changed to 3.0. (A) B1 and B2; (B) B3 and B3'; (C) D1 and D2.

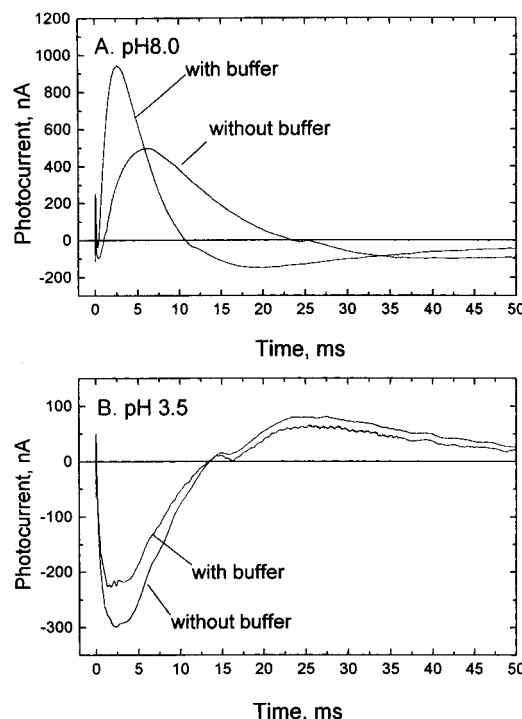
optical excitation conditions. These results suggest a possible correlation between B3 and D1. Furthermore, it is found that the signs of B1 and B2 depend on the film orientation, whereas those of B3 and D1 do not.<sup>16</sup>

**3.2. The pH Dependence of B3 and B2.** Figure 3A shows the pH dependence of B2 under pulsed laser excitation. Within a wide pH range from 1.0 to 11.0, no polarity change is observed for B2. The area of B2 decreases to zero rapidly at pH >10.5 and pH <2.0. This is mainly due to the low efficiency in proton pumping, as well as denaturation of purple membrane under these extreme conditions. A detailed discussion has been given in a previous study.<sup>25</sup> Parts B and C of Figure 3 show the pH dependence of B3 and D1, respectively. The polarity reversal of B3 occurs around pH 5.5. At this pH region, the B3 component is extremely small. As the pH increases, B3 increases and reaches a maximum value at pH ~8.5 and decreases at even higher pH. As pH goes below 5.5, B3 reappears with an opposite sign and reaches a minimum at pH ~3.0. The pH dependence of D1 parallels that of B3, suggesting that their origins are the same. The integrated area ratio of the B3 to the B2 components in Figure 3 changes as a function of pH. It is as high as ~80 at pH 9.0, almost zero around pH 5.5, and about -30 at pH 3.5.

**3.3. The Effect of pH Buffer and Ionic Strength on B3.** The origin of B3 is not a result of a buffer effect. The presence of a buffer, however, does affect the waveform of B3. Figure 4 shows the effect of buffer on B3, measured in 10 mM KCl, pH 8.0 and 3.5 (with and without 2 mM K<sub>2</sub>HPO<sub>4</sub> buffer). It can be seen that the buffer effect on B3 is different when measured at different pH values. At pH 8.0, the waveform of B3 changes significantly upon the addition of the buffer, in both

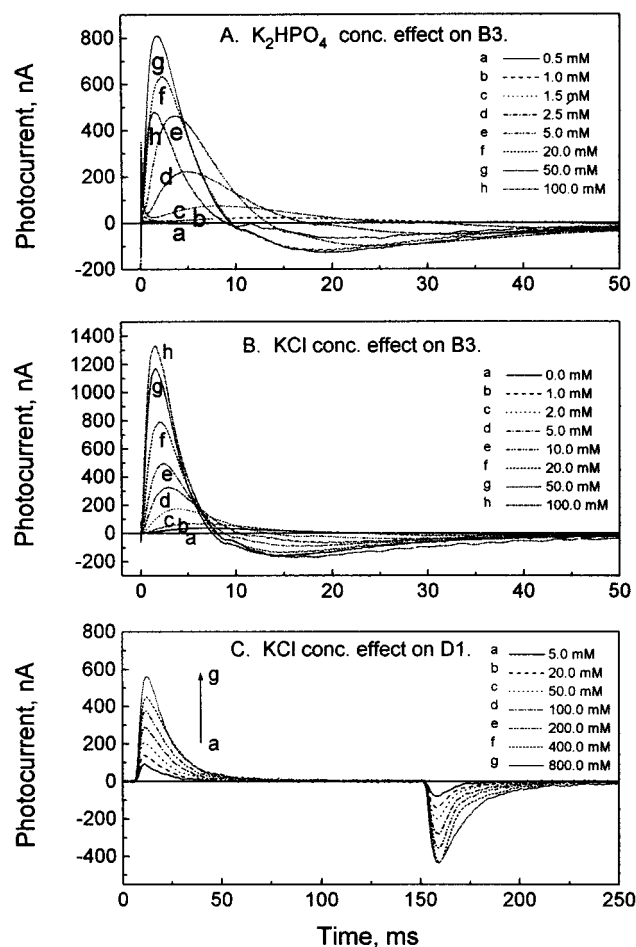


**Figure 3.** pH dependence of the integrated areas under the photocurrent measured in 10 mM KCl and 1.5 mM K<sub>2</sub>HPO<sub>4</sub>. The pH is adjusted by addition of several microliters of 1 M KOH or HCl. A, B, and C are for B2, B3, and D1, respectively. The similarity of the pH dependence of B3 and D1 is clearly shown.



**Figure 4.** Effect of buffer on the rise and decay of B3 at pH = 8.0 and 3.5. The addition of buffer (10 mM KCl and 2 mM K<sub>2</sub>HPO<sub>4</sub>) leads to an increase in both the rise and decay of the photocurrent.

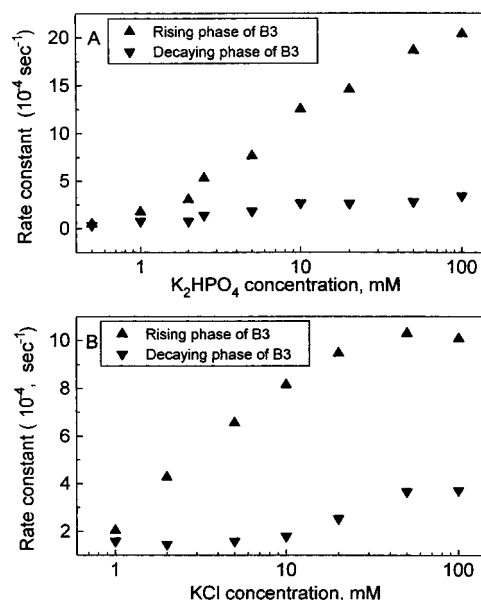
magnitude and lifetime. At pH 3.5, however, the peak position of B3 is essentially the same with or without the buffer, but the photocurrent signal is negative. In addition, the presence of the pH buffer at pH 3.5 causes B3 to decrease in magnitude. The buffer effect could be reproduced by washing out and re-adding the buffer. A similar pH dependence was observed when 5 mM CaCl<sub>2</sub> is used as the electrolyte (data not shown).



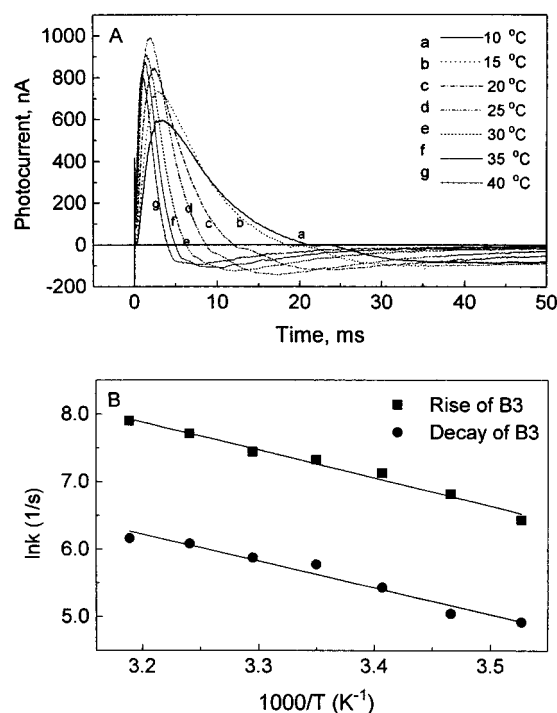
**Figure 5.** Effect of ionic strength on the rise and decay of B3 and D1. (A) Effect of buffer concentration at pH 8.0; (B) KCl concentration effect on B3, in 1 mM  $K_2HPO_4$ ; and (C) KCl concentration effect on D1/D2, in 1 mM  $K_2HPO_4$  at pH 8.5. It is shown that the addition of an electrolyte increases the rate of the rise and decay of two signals, as well as the integrated charge transferred.

Figure 5A shows the effect of buffer concentration on B3 at constant pH. At low buffer concentration, B3 decays slower and is smaller in amplitude. As the pH buffer is added, the rise time becomes shorter and the peak magnitude increases until 50 mM buffer is added. Then the amplitude of B3 starts to decrease when the buffer concentration reaches 100 mM. As B3 changes, B3' also changes its shape and shifts its peak position. Figure 5B shows B3 as a function of the KCl concentration at a constant concentration of buffer (1 mM  $K_2HPO_4$ , pH 8.0). The amplitude of B3 increases as the ionic strength is increased between 1.0 and 100 mM KCl. A similar ionic strength effect on B2 was reported previously.<sup>25</sup> The saturation observed in the amplitude of B3 on buffer concentration is consistent with the proposal that B3 is related to the local pH change near the ITO/bR interface. When the buffer concentration exceeds a certain value, the pH change due to the proton pumping is expected to become smaller due to the buffering ability of the solution. As a result, B3 decreases its amplitude.

Figure 5C shows the effect of KCl concentration on D1 and D2. As can be seen, the amplitude of D1 increases as the electrolyte concentration increases. No saturation is observed up to 800 mM KCl. Similar results are also obtained for B3 and B3', as well as D1 and D2, when various other electrolyte solutions (KCl, NaCl,  $Na_2SO_4$ , and  $CaCl_2$ ) are used with and without pH buffer. It should be pointed out that a much smaller B3 is observed for an oriented bR gel<sup>9</sup> than what we report in



**Figure 6.** Effect of buffer ( $K_2HPO_4$ , A) and ionic strength (KCl, B) on the rate constant of the rise and decay of B3.



**Figure 7.** (A) Dependence of the photocurrent B3 on temperature. (B) Arrhenius plots of its rise (■) and decay (●) rate constants measured in a solution of 20 mM KCl, 2 mM  $K_2HPO_4$  at pH = 8.0.

this paper. This is most likely due to the different sample geometry used in the oriented bR gel. In our experiment, the ITO electrode is in contact with the oriented bR film while in their oriented gel experiment, the bR gel was separated away from the Pt electrodes.<sup>14</sup>

The fastest rate constant of the rising phase in B3 is found to be  $\sim 2 \text{ m s}^{-1}$ , and the fastest decay constant is  $\sim 0.4 \text{ m s}^{-1}$  in  $\sim 100 \text{ mM}$  buffer (pH 8.0). Figure 6A shows the rate constants for the rise and decay of B3 as a function of buffer concentration at pH 8.0. It can be seen that an increase in rate constants for both the rise and decay of B3 is observed as the buffer concentration increases. The effect of KCl concentration on the rate constants of the rise and the decay of B3 is shown in Figure 6B.

### 3.4. The Temperature Dependence of the Photocurrent.

Figure 7A shows the temperature dependence of B3 at constant electrolyte and buffer concentration (20 mM KCl, 2 mM K<sub>2</sub>-HPO<sub>4</sub>) at pH 8.0. A significant shift in the peak position of B3 is observed when the temperature is changed. Figure 7B shows the Arrhenius plots of the rate constants for the rising phase and decaying phase of B3. The activation energy ( $E_a$ ) and frequency factor ( $A$ ) for B3 are determined to be 8.3 kcal mol<sup>-1</sup> and  $1.56 \times 10^9$  s<sup>-1</sup> for the rising phase and 7.9 kcal mol<sup>-1</sup> and  $1.65 \times 10^8$  s<sup>-1</sup> for the decaying phase, respectively. The activation energies of both the rise and the decay of B3 are close to that of B2 component, and the frequency factors are much smaller than that of B2 reported<sup>9</sup> previously ( $E_a = 13.5 \pm 0.2$  kcal mol<sup>-1</sup> and  $A = 1.65 \times 10^{14}$  s<sup>-1</sup>).

## 4. Discussion

**4.1. Origin of the B3 and D1 Components.** It is generally believed that B1, the pH-insensitive photocurrent, is generated by light-induced intermolecular charge separation due to the photoisomerization of the retinal chromophore.<sup>7-9,12,26</sup> B2 has the same direction as the vectorial proton transfer<sup>8,9</sup> and is assigned to the proton pumping during the L  $\rightarrow$  M transition. Our results reported here suggest that B3 originates from the change in proton concentration near the ITO/bR interface as a result of the bR photocycle. This is consistent with the conclusions of recent studies comparing the D1 and B3 components,<sup>16</sup> as well as a previous paper on the differential photocurrent.<sup>20</sup>

The fact that B3 has a rise time slightly slower than the decay of B2 at high pH, as well as slower than the M formation, is consistent with the proposal that B3 results from the creation of a proton concentration gradient during the photocycle of bR. Several pieces of evidence suggest that B3 is due to the local proton release/uptake, which determines the polarity of the signal at different pH values. First, the B3 component is always cathodic at high pH whereas anodic at low pH. Second, the rise time of the B3 can be as short as several hundred microseconds, if a pH buffer or an electrolyte solution is added. This rise time is in good agreement with the result from the proton release study that used pH-indicator dye located in the bulk solution.<sup>27</sup> And finally, B3 is the same for oriented or nonoriented bR film (our unpublished data) but B1 and B2 are different, further supporting that B3 and D1 originate from the proton uptake/release near the ITO/bR interface, but not from the vectorial proton or ion transportation.

Upon light excitation, a proton is transferred from the protonated Schiff base of bR to D85 within the membrane during L  $\rightarrow$  M transition. At approximately the same time, a proton appears on the extracellular surface and creates a pH gradient across the membrane. The protons either stay on the membrane surface<sup>28</sup> or are released locally into the bulk solution near the membrane-ITO interface. At pH > 6, proton release precedes proton uptake, the release on the extracellular side occurs approximately during the rise of M, and the re-uptake on the cytoplasm side occurs roughly at the decay of N.<sup>28</sup> At pH < 5, bR first gains, instead of loses, a proton during the photocycle.<sup>28-30</sup> As a result of the change in the pH near the ITO/bR interface due to the proton uptake or release, a transient pH change results. This pH change produces transient voltage on the bR-containing ITO electrode. This gives rise to the observed photocurrent: a pH decrease generates a positive photocurrent, and a pH increase generates a negative photocurrent. The sign of the photocurrent (B3 and D1) is thus only determined by the sign of the local pH change, but not by the orientation of the bR film near the ITO/bR interface. The positive and negative

ions in solution will respond to the two electrodes by moving in opposite directions. This causes the decay of the observed photocurrent.

Here we introduce  $\Delta[H^+]/\Delta t$  to describe the local transient change in proton concentration near the bR-ITO interface. At high pH, the increase in the proton concentration near the bR-modified ITO interface generates a transient cathodic photocurrent because  $\Delta[H^+]/\Delta t$  is > 0. The H<sup>+</sup> concentration change can be detected by the chemical capacitor consisting of the electrode pair. The counterion movement in the electrolyte solution bathing the ITO electrode leads to the decay of this transient photocurrent. However, the uptake of proton might also contribute to the decay of B3. The discharging process of the chemical capacitor leads to the B3' signal. The disappearance of the protons taken up by bR during its photocycle at low pH explains the anodic property of B3, since  $\Delta[H^+]/\Delta t$  is < 0. Decrease in the photocurrent at even lower pH indicates a less efficient proton pumping process, whereas at near neutral pH regions  $\Delta[H^+]/\Delta t \approx 0$ , because the average proton release and proton uptake give no significant transient change in the net proton concentration. Increasing [H<sup>+</sup>] at the ITO/bR local domain gives positive (or cathodic) current, and decreasing [H<sup>+</sup>] causes negative (or anodic) current. This model can also explain the differential photocurrent obtained using CW light, since D1 can be obtained from the time-integral of B3 on millisecond time scale.

The membrane orientation affects the polarity of both the B1 and B2 components, since these are intramembrane charge separation processes. When bR is oriented with the extracellular surface facing the ITO electrode, the vectorial proton transfer from the cytoplasmic side to the extracellular side should produce a negative photocurrent, as observed.<sup>16</sup> On the contrary, the membrane orientation does not affect the polarity of B3, since the change in the proton concentration rapidly equilibrates at the membrane-ITO interface and the proton concentration near the ITO interface is not affected by the orientation of the bR molecules. Cathodic B3 occurs only when the net proton concentration increases near the ITO/bR interface, and anodic B3 is observed only when the net proton concentration decreases near the ITO/bR interface.

The pH effect on the proton release has been suggested to correlate with the protonation state of the unknown amino group XH, possibly R82.<sup>28</sup> In the mutant R82Q, in which the arginine is replaced with glutamine, the proton release near pH 7 is changed into a delayed proton uptake.<sup>30,31</sup> Our results show that this proton uptake process in R82Q is reflected in the differential photocurrent: an anodic D1 current as well as a B3 is observed at pH 7 (data not shown here), which is similar to that of native bR at pH < 5. Furthermore, our model is also supported by the pH change study in the aqueous phase of bR-containing vesicles.<sup>32</sup> It was reported that purple membrane showed a net proton release into the solution at high pH and a net proton uptake at low pH, which is consistent with the observed pH dependence in this study for both B3 and D1 (Figure 3B,C).

The origin of the polarity change in the differential photocurrent is mostly due to B3, which changes its polarity at high pH versus low pH. The direction of proton pumping, however, is pH-independent; it always goes from the CP side to the EC side. No correlated spectroscopic intermediate has been identified in the photocycle of bR for the time scale of B3, although it is within the photocycle time ( $\sim 10$  ms). Our results indicate that the origin of D1 in the differential photocurrent is the same as that of B3.<sup>16</sup> This assignment is different from those reported previously.<sup>17,18,33</sup>

**4.2. Factors That Affect the B3 as Well as the D1 Components.** When we first observed the slow component B3 at high pH, such as shown in Figure 1B, we thought that it could be due to a buffer effect or some artificial effect on the measuring system. As reported in Liu's work,<sup>34</sup> the waveform of B2 is altered when a pH buffer is added. The 31 types of buffer that were studied show either positive or negative effects on the decay of B2. We find, however, that B3 is not a pH-buffer-induced component, since it also exists in the absence of a buffer (Figure 4). At pH  $\sim$ 6.0, in 5 mM CaCl<sub>2</sub>, a small trace of B3 has been observed.<sup>9</sup> We believe that the reason that a strong B3 was not observed by them was due to the different electrode geometry used as well as the pH. From Figure 3B, it can be seen that B3 is very small near pH 6. In addition, the amplitude of B3 is substantially increased by the addition of a pH buffer (Figures 4A and 5A) and leads to a partial overlap with the B2 decay. A nonbuffer type electrolyte shows a similar acceleration effect on B3 (Figure 5B). The acceleration of B3 is mainly due to kinetic reasons. Under low ionic strength, the transfer of protons from the membrane surface to the bulk is delayed in the bound water layer near the membrane. The exchange of protons between the bulk and interfacial solution is measurably accelerated when a buffer is added.<sup>35,36</sup> This fact can be used to explain the increase in the rising rate of B3 in the presence of a buffer or salt. A similar conclusion can also be drawn from previous pH-indicator dye studies.<sup>27,37</sup> With the addition of more and more electrolyte into the bathing solution, besides the acceleration of the change in proton concentration at the interface due to the increase of the ionic strength, an acceleration in the decay kinetics takes place as a result of the faster response of the counterions to neutralize the polarized electrodes.

For the case of high buffer concentration, the function of the buffer should be considered, in addition to the increase in the ionic strength. The buffering action of a pH buffer solution depends on its concentration. The observed proton concentration change due to the proton release or uptake processes will be affected by the presence of a high concentration of pH buffer. The amount of unprotonated buffer molecules exceeds the population of protonated ones at pH  $>$  pK<sub>a</sub> of a buffer, and vice versa at pH  $<$  pK<sub>a</sub>. At low pH, the buffer is protonated, and therefore the loss of proton from solution is less favorable than that at high pH, which leads to the decrease in the magnitude of B3 in the presence of a pH buffer. This supports the proposal that B3 is related to the proton concentration changes near the bR-ITO electrode. When the buffer concentration exceeds a certain value, the local pH change near the ITO/bR interface is reduced. This would explain the decrease in B3 and D1 when the buffer concentration exceeds 50 mM.

It should be pointed out that there is mainly a buffer effect on B3 in the millisecond time domain, rather than only on B2, as previously concluded.<sup>34</sup> Further, the pH dependence of the B3 component determines the behavior of the buffer effect. Liu et al.<sup>34</sup> showed in their paper that the buffer effect starts to appear at pH =  $5.8 \pm 0.3$  and ends at pH =  $8.2 \pm 0.3$ . This agrees well with the behavior of B3 we observed in this pH region (Figure 3B).

## 5. Conclusion

The photocurrent from an oriented bacteriorhodopsin film immersed in an electrolyte solution in various time regions has been studied under both pulsed and CW laser excitations. Several components, B1, B2, B3 (B3') as well as D1 and D2, have been examined. B3 and D1 are pH-dependent in the pH range 1.0–11.6. B3 and D1 are cathodic at high pH, are very

small at pH 5–6, and become anodic at lower pH. The change in polarity of B3 and D1 as a function of pH can be understood based on a mechanism that attributes the photocurrent to transient changes in the proton concentration during the photocycle of bR. This proton concentration gradient results from proton release or uptake, as a result of the bR photocycle, in the local aqueous domain near the ITO/bR interface. A positive photocurrent is observed when the local pH near the ITO/bR interfaces decreases, and a negative signal is observed when the local pH increases. The proton-transfer process results in a proton concentration gradient and thus a voltage difference between the two electrodes giving rise to the observed photocurrent. The decay of the photocurrent results from the response of the ions in solution to the photoinduced polarization at the two electrodes.

**Acknowledgment.** The authors wish to thank the support of the Department of Energy for this work under DOE-FG03-88ER13828. We would also like to thank Professor J. K. Lanyi for providing the R82Q mutant. In addition, we would like to thank Tina M. Masciangioli and Janet M. Petroski for proof-reading the manuscript.

## References and Notes

- (1) Oesterhelt, D.; Stoekenius, W. *Nature New Biol. (London)* **1971**, 233, 149.
- (2) Mathies, R. A.; Lin, S. W.; Ames, J. B.; Pollard, W. T. *Annu. Rev. Biophys. Chem.* **1991**, 20, 491.
- (3) Birge, R. R. *Annu. Rev. Phys. Chem.* **1990**, 41, 683.
- (4) Lanyi, J. K. *Biochim. Biophys. Acta* **1993**, 1183, 241.
- (5) Ebrey, T. G. *Light Energy Transduction in Bacteriorhodopsin*; CRC Press: London, 1993.
- (6) Keszthelyi, L.; Ormos, P. *FEBS Lett.* **1980**, 109, 189.
- (7) Keszthelyi, L.; Ormos, P. *Biophys. Chem.* **1983**, 18, 397.
- (8) Holz, M.; Lindau, M.; Heyn, M. P. *Biophys. J.* **1988**, 53, 623.
- (9) Liu, S. Y. *Biophys. J.* **1990**, 57, 943.
- (10) Trissl, H. W. *Photochem. Photobiol.* **1990**, 51, 793.
- (11) Trissl, H. W. *Biophys. J.* **1987**, 52, 141.
- (12) Liu, S. Y.; Ebrey, T. G. *Photochem. Photobiol.* **1987**, 46, 263.
- (13) Ormos, P.; Hristova, S.; Keszthelyi, L. *Biochim. Biophys. Acta* **1985**, 809, 181.
- (14) Liu, S. Y.; Ebrey, T. G. *Biophys. J.* **1988**, 54, 321.
- (15) Boucher, F.; Taneva, S. G.; Elouatik, S.; Dery, M.; Messaoudi, S.; Harvey-Girard, E.; Beaudoin, N. *Biophys. J.* **1996**, 70, 948.
- (16) Wang, J.-P.; Yoo, S.-K.; Song, L.; El-Sayed, M. A. *J. Phys. Chem. B* **1997**, 101, 3420.
- (17) Miyasaka, T.; Koyama, K.; Itoh, I. *Science* **1992**, 255, 342.
- (18) Koyama, K.; Yamaguchi, N.; Miyasaka, T. *Science* **1994**, 265 (5173), 762.
- (19) Wang, J. P.; Li, J. R.; Taxo, P. D.; Li, X. C.; Jiang, L. *Adv. Mater. Opt. Electron.* **1994**, 4, 219.
- (20) Robertson, B.; Lukashev, E. P. *Biophys. J.* **1995**, 68, 1507.
- (21) Becher, B.; Cassium, J. Y. *Prepr. Biochem.* **1975**, 5, 161.
- (22) Varo, G. *Acta Biol. Acad. Sci. Hung.* **1981**, 32, 301.
- (23) McIntosh, A. R.; Boucher, F. *Biochim. Biophys. Acta* **1991**, 1056, 149.
- (24) Butt, H. J.; Fendler, K.; Bamberg, E.; Tittor, J.; Oesterhelt, D. *EMBO J.* **1989**, 8, 1657.
- (25) Liu, S. Y.; Govindjee, R.; Ebrey, T. G. *Biophys. J.* **1990**, 57, 951.
- (26) Rayfield, G. W. *Biophys. J.* **1983**, 41, 109.
- (27) Heberle, J.; Oesterhelt, D.; Dencher, N. A. *EMBO J.* **1993**, 12, 3721.
- (28) Lanyi, J. K. *J. Bioenerg. Biomembr.* **1992**, 24, 169.
- (29) Dencher, N. A.; Wilms, M. *Biophys. Struct. Mech.* **1975**, 1, 259.
- (30) Zimanyi, L.; Cao, Y.; Needleman, R.; Ottolenghi, M.; Lanyi, J. K. *Biochemistry* **1993**, 32, 7669.
- (31) Otto, H.; Marti, T.; Holz, M.; Mogi, T.; Stern, L. J.; Engel, F.; Khorana, H. G.; Heyn, M. P. *Proc. Natl. Acad. Sci. U.S.A.* **1990**, 87, 1018.
- (32) Takeuchi, Y.; Ohno, K.; Yoshida, M.; Nagano, K. *Photochem. Photobiol.* **1981**, 33, 587.
- (33) Miyasaka, T.; Koyama, K. *Thin Solid Films* **1992**, 210–211, 146.
- (34) Liu, S. Y.; Kono, M.; Ebrey, T. G. *Biophys. J.* **1991**, 60, 204.
- (35) Drachev, L. A.; Kaulen, A. D.; Skulachev, V. P. *FEBS Lett.* **1984**, 178, 331.
- (36) Grzesiek, S.; Dencher, N. A. *FEBS Lett.* **1986**, 208, 337.
- (37) Scherrer, P.; Alexiev, U.; Otto, H.; Heyn, M. P.; Marti, T.; Khorana, G. H. *Colloq. INSERM* **1992**, 221, 205.